Piezoelectric properties of polymer/lead-free ceramic composites

Mike Alexandre, Camille Bessaguet, Charlotte David, Eric Dantras, Colette Lacabanne

http://dx.doi.org/10.1080/01411594.2016.1206898

Piezoelectric properties of polymer/lead-free ceramic composites

M. Alexandre*, C. Bessaguet*, C. David**, E. Dantras and C. Lacabanne

Physique des Polymères, Institut Carnot CIRIMAT, Université Toulouse 3- Paul Sabatier, Toulouse, France

ABSTRACT

Thermoplastic/lead-free piezoelectric ceramic composite have been prepared. Sodium niobate ($NaNbO_3$) has been chosen for its high Curie temperature. Moreover, it could be synthesized with two different morphologies: $NaNbO_3$ nanowires (NN NW's) and $NaNbO_3$ particles (NN P's). The filler has been dispersed in thermoplastic matrices with different dielectric permittivities ε_M: PA11 ($\varepsilon_M = 2$) and polyvinylidene fluoride (PVDF) ($\varepsilon_M = 10$). Due to polarization conditions, only ceramic particles are poled. The piezoelectric coefficient (d_{33}) has been measured in composites. The higher d_{33} is recorded in composites based on PA11 ($d_{33} = 6.5$ $pC.N^{-1}$ for 30 vol. % NN NW's). The influence of the NN aspect ratio on PVDF/NN composites has been analysed: the higher d_{33} ($d_{33} = 2.6$ $pC.N^{-1}$ for 25 vol. %) is recorded in PVDF/NN P's. The major interest of these hybrid lead-free piezoelectric composites is mild poling conditions, ductility and thermal stability of piezoelectric performances.

KEYWORDS

Lead-free ceramic; sodium niobate; polymer/piezoelectric ceramic composite; thermoplastic polymer; nanowire; aspect ratio

Introduction

In the last few decades, much attention has been given to the study of organic ferroelectric materials.[1−9] These electroactive polymers are very attractive because of their light weight, easy moulding and good piezo/pyroelectric properties. In sensor applications, the low dielectric properties of polymers enable them to reach higher piezoelectric performances than those obtained for conventional piezoelectric ceramics. However, in order to obtain the ferroelectric properties,[10] these organic materials require a poling field 10 times higher than conventional ferroelectric ceramics,[11,12] sometimes leading to dielectric breakdown. Moreover, the low thermal stability of the piezoelectric properties of ferroelectric polymers limits their applications.[13,14] In some particular cases, it is required to preserve, on the one hand, easy processing and mechanical properties of polymers and, on the other hand, the thermal stability of piezoelectric ceramics.[5,15,16] Many works have reported the elaboration and characterization of polymers/inorganic piezoelectric particles composites.[17−23] The studied particles generally had poor thermal stability (e.g. $BaTiO_3$). Moreover, some were prepared from toxic and non-environmentally friendly precursors e.g. lead titanate zirconate (PZT).[24−26]

Since 1997, regulations [27] on the use of lead have resulted in more research about lead-free ferroelectric ceramics such as sodium niobate ($NaNbO_3$/NN). $NaNbO_3$ is a ferroelectric ceramic with seven crystalline phases named N, P, R, S, T1, T2 and U, depending on the phase it can be ferroelectric, antiferroelectric or paraelectric.[28−33] The most interesting phase transition is the P−R

CONTACT C. Lacabanne colette.lacabanne@univ-tlse3.fr

* Present address: Institut de Recherche Technologique (IRT) Saint Exupéry, 118 route de Narbonne, CS 44248, 31432 Toulouse cedex 4, France

** Present address: Airbus Helicopters, A´eroport de Marseille Provence, 13700 Marignane, France

transition that can be considered as the Curie transition. According to the literature, it takes places at a high temperature: 360 °C−370 °C).[31,32] In 2003, Goh et al. [34] were the first to synthesize $NaNbO_3$ in powder form using a hydrothermal synthesis method. Few years later, Zhu et al. [35] showed that the structure and composition of $NaNbO_3$ depended on temperature and time. With a classical protocol of hydrothermal crystallogenesis, either particles (NN P's) or nanowires (NN NW's) can be synthesized in the laboratory. Ceramic nanowires have been synthesized in many works.[36−39] Nevertheless, it appears to be quite difficult to preserve a non-centrosymmetric crystalline cell that is crucial for ferroelectric structure.[40−42] More recently, Sodano et al. showed that the use of piezoelectric nanowires instead of particles can lead to an increase of final piezoelectric properties of composites.[43]

In 2012, David et al. [44] elaborated a thermoplastic polymer (PA11)/NN NW's composite to study its piezoelectric properties. Note that only ceramic particles were polarized due to low poling fields. They highlighted the influence of the ceramic permittivity on the polarization step and, therefore, the piezoelectric coefficient. Following this line of reasoning, in this study, thermoplastic polymer/NN piezoelectric particles composites were investigated. Polymer matrices with different permittivities were chosen: PA11 with a permittivity of 2, in the vitreous state at room temperature (RT) [44] and polyvinylidene fluoride (PVDF) with a permittivity of 10, in the rubbery state at RT. [45] In the oriented state, these polymer matrices can be piezoelectric after poling by fields of up to 100 $kV.mm^{-1}$, for a duration of about 1 h. Ploss et al. [46] studied PVDF-TrFE/PZT composites: under a field of 55 $kV.mm^{-1}$ during 1 h, the copolymer matrix remains unpoled, only ceramic inclusions were polarized. In this study, the 'low' electric field applied (10 $kV.mm^{-1}$) leads only to the polarization of the ferroelectric ceramic. As a result additional contributions can be avoided (e.g. Maxwell−Wagner−Sillars or interfacial polarization between crystalline and amorphous phases of the polymer). PA11 and PVDF were used as structural matrices of the composites. We will focus on the influence of the aspect ratio of NN NW's and NN P's piezoelectric particles as well as the dielectric permittivity of the matrix on the piezoelectric coefficient (d_{33}) of the composites.

Experimental section

Synthesis of $NaNbO_3$

$NaNbO_3$ (or NN) was synthesized by hydrothermal crystallogenesis.[34,35,44] Niobium pentoxide (Nb_2O_5) and concentrated (10 M) sodium hydroxide (NaOH) were mixed and dispersed for 1 min in an ultrasonic bath. Then, the mixture was transferred to an autoclave and heated at 183 °C. Nb_2O_5 powders aggregate and grow to form irregular bars. Depending on the time of reaction, different morphologies are obtained; nanowires (NW's) are obtained after almost 2 h of reaction and particles (P's) are formed after 8 h of reaction. For both forms, an intermediate compound is obtained after the reaction: $NaNb_6O_{15}OH$.[44] Rinsing with deionized water removes the sodium hydroxide and neutralizes the pH. Then, an annealing at 600 °C for 6 h was performed to obtain NN P's or NN NW's.

Figure 1 represents scanning electron microscopy (SEM) images (SEM-FEG JEOL JSM-6700F) of NN NW's (a) and NN P's (b). NW's are about 50 μm long with a diameter of about 500 nm. Particles are cubic with a lateral size of about 1 μm.

Elaboration of $NaNbO_3$ ceramic

In order to determine the Curie temperature, a disk of bulk NN was processed by pressing and sintering. Spark plasma sintering (SPS) was used to limit the grain growth. The temperature was increased from RT until 1000 °C at 100 °C/min. Finally, the sample was annealed under oxygen atmosphere for a few hours to reduce the residual carbon on the sample surface.

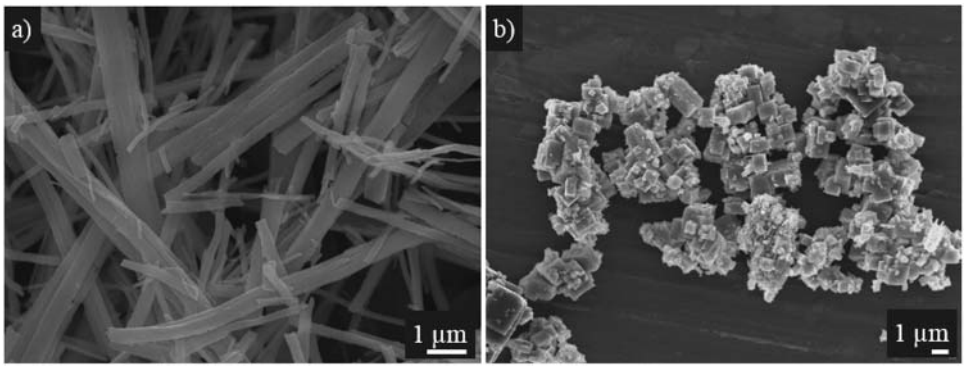

Figure 1. SEM images of NN NW's (a) and NN P's (b).

Polymer/$NaNbO_3$ composites processing

PA11/NN composites were elaborated according to the protocol described in [44]. PA11 was dissolved in a mixture of dichloromethane and formic acid. Then, NN powder was dispersed in the solution. Finally, the dispersion was poured into water and the PA11/NN composite precipitated.

For PVDF/NN composites, PVDF and NN powders were mixed in ethanol. The suspension was dispersed by ultrasound for a few minutes. Then, the ethanol was evaporated to obtain a homogeneous composite powder. The powder was dried at 100 °C in order to completely remove all traces of ethanol.

The processing of films was performed using an extruder at 200 °C. The dispersion in composites with a volume fraction of 20% of NN NW's and NN P's is shown in Figure 2. The dispersion is very important to observe homogeneous piezoelectric properties at the macroscopic scale. The nanowire dispersion is homogeneous even if some aggregates are visible due to the high aspect ratio. As expected, the dispersion of particles is better due to their morphology.

Methods

Polarization protocol

The polarization step consists of applying a high static electric field to the sample in order to allow the orientation of electric dipoles.[19,45,47] It is a critical step to obtain a piezoelectric composite.

Two parameters were optimized: electric field and temperature. The electric field must be higher than the coercive field of the NN, i.e. 2.2 kV/mm.[48] The temperature has to be higher than the

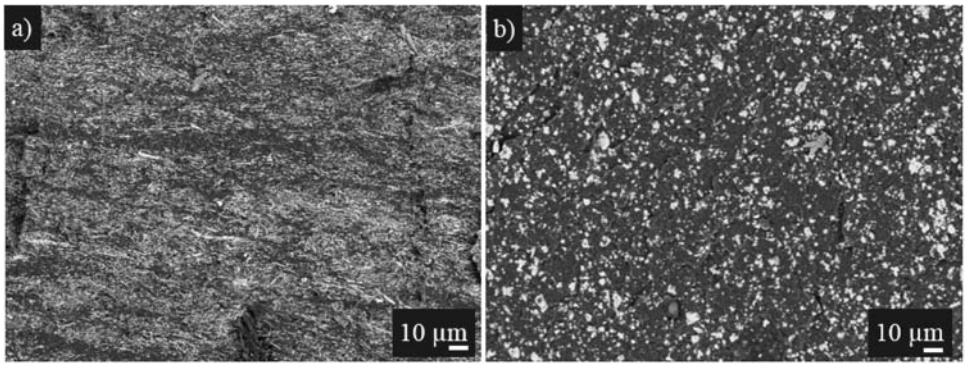

Figure 2. SEM images of PVDF/20 vol. % NN cryocuts: (a) nanowires and (b) particles.

glass transition of the polymer to increase the matrix permittivity. The composite was polarized at 110 °C under a static electric field of 10 kV.mm^{-1} during 15 min. Samples were immersed in an oil bath to avoid breakdown.

Piezoelectric measurements

The piezoelectric coefficient (d_{33}) measurements were carried out 24 h after the polarization step to avoid effects of the electric charges accumulated on the composite surface.

The piezoelectric coefficient was measured by a PM 200 piezometer supplied by Piezotest (UK). Frequency and stress were set to 110 Hz and 0.25 N, respectively. The stress was applied to the sample in the same direction as the polarization and the amount of electric charges created was measured.

Results and discussion

$NaNbO_3$ characterization

X-ray diffraction

X-ray diffraction (XRD) analysis was performed on the NN at RT every 0.02 °/s to measure the crystal lattice parameters and confirm the presence of NN. Figure 3 shows the XDR pattern of NW's (Figure 3(a)) and P's (Figure 3(b)). In both cases, the pattern has the same peaks which correspond to the orthorhombic crystalline phase (*Pbma*) of the NN (JCPS 89-8957). According to the literature, however, NN is in its P phase at RT, which means it has an orthorhombic network with the spatial group *Pbcm*. This difference could be due to the measurement uncertainty because the peaks at 36.5° and 38.5° are not entirely resolved.

In order to highlight the NN phase transitions, a XRD analysis was performed on the ceramic powder at temperatures ranging from 30 °C to 800 °C. Patterns are shown in Figure 4. There is no evolution of the crystalline structure between 30 °C and 600 °C, so these thermograms are not presented here. The evolution of the crystalline structure can be divided into three regions. From 30 °C to 650 °C, the presence of two diffraction peaks indicates that the structure of NN is orthorhombic. At 700 °C, a new diffraction peak is observed: it corresponds to the tetragonal structure (*P4/mbm*) according to JCPS 89-6654 data. Then, from 700 °C to 800 °C, the crystalline structure is cubic (*Pm3m*).

Curie temperature

Due to the complexity of NN structures, a lot of works have been devoted to the study of transitions. [29−33,48,49] The P−R transition temperature (T_{P-R}) has generally been associated with the Curie

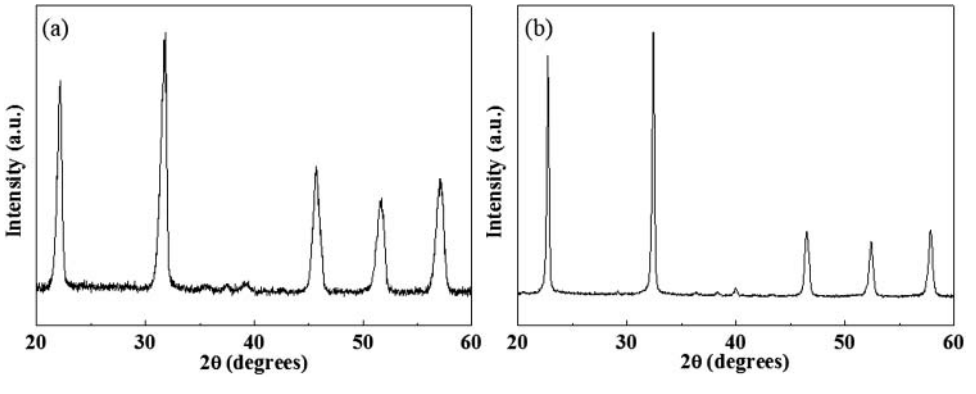

Figure 3. XRD patterns of NN NW's (a) and NN P's (b) at RT.

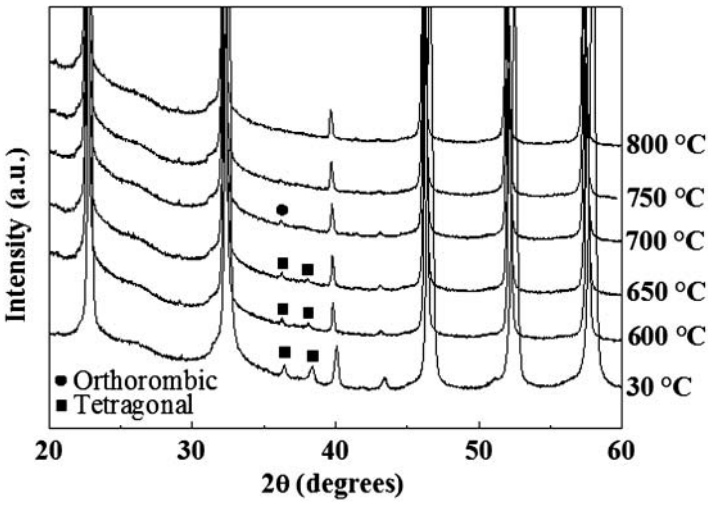

Figure 4. XRD patterns of NN powder at different temperatures. (■) and (●) represent the tetragonal and orthorhombic crystalline structure, respectively.

temperature. In the case of NN, the T_{P-R} is too high and the modifications in the lattice parameters too small, making it impossible to detect this transition by differential scanning calorimetry (DSC) and XRD. Therefore, a non-classical protocol has been developed to determine the Curie temperature of the particles synthesized in the laboratory. A bulk ceramic disk was manufactured, poled and annealed at different temperatures. Figure 5 represents the evolution of d_{33} (%) of the bulk ceramic as a function of annealing temperature. The d_{33} maximum value is measured at 34.5 $pC.N^{-1}$, which is in agreement with values found in literature.[48,49] It is interesting to note that the transition, measured at 287 °C, is spread out over a wide temperature range (from 265 °C to 310 °C). This could be explained by the influence of the NN grain size on the P−R transition according to Moure et al. [31]. In this work, for a particle size lower than 70 nm, the transition temperature is 180 °C. For a particle size between 200 and 400 nm, the transition temperature is between 310 °C and 330

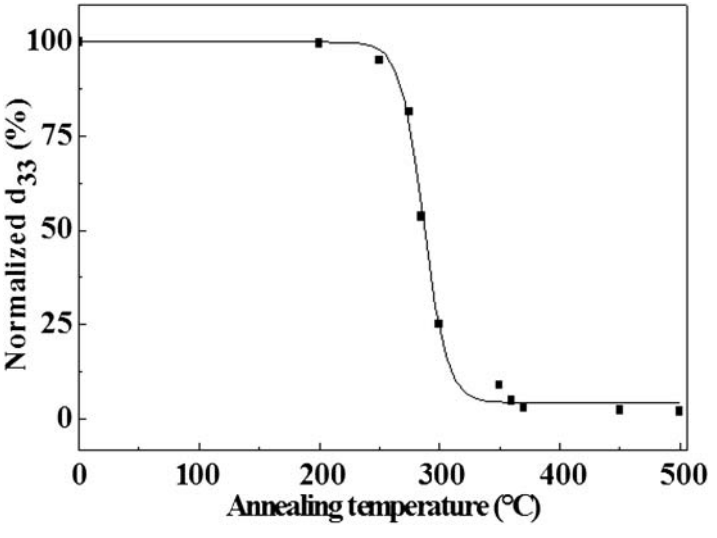

Figure 5. Variation of the normalized piezoelectric coefficient (d_{33}) of the NN ceramic according to the annealing temperature. The line is just a guide for the eyes.

°C; finally, for particles larger than 1 μm, the transition temperature is 370 °C. On the other hand, Molak et al. [33] measured this P−R transition between 343 °C and 370 °C for monocrystalline samples. In our case, the dispersion of the particle size is important and NN is polycrystalline. This could explain the difference in the T_{P-R} value, the broad transition of d_{33} and the lag of transition temperatures measured by XRD.

Matrix influence

Figure 6(a) represents the variation of d_{33} of polymer/NN NW's composites versus the volume fraction of NN NW's, for PA11 and PVDF matrix, respectively. As expected, in both cases, d_{33} increases with the fraction of NN. The increase is more pronounced in the case of PA11 composites: for 20 vol. % of NN NW's, $d_{33} = 2.9$ pC.N^{-1} while $d_{33} = 0.8$ pC.N^{-1} for PVDF composites. In addition, a piezoelectric coefficient d_{33} of 6.5 pC.N^{-1} is reached for a PA11/30 vol. % NN NW's composite.

During the polarization, the real electric field that is applied to the ceramic depends on the matrix permittivity and can be calculated from the Equation (1) [50]

$$\vec{E}_{NP} = \frac{3\varepsilon_M}{\varepsilon_{NP} + 2\varepsilon_M}\vec{E}_{appl} \quad (1)$$

where $\vec{E}_{NP}$ is the real electric field applied to the particles, ε_M and ε_{NP} are the matrix and particle dielectric permittivity, respectively, and $\vec{E}_{appl}$ is the applied electric field.

The polarization efficiency (and, therefore, the piezoelectric coefficient) is directly linked to the real electric field applied to the ceramic which in turn depends on the matrix permittivity. However, PA11 and PVDF permittivity are 2 [44] and 10,[45] respectively. Therefore, PVDF composites get a higher polarization than PA11 composites. But since the amorphous PVDF phase is in the rubbery state at RT, part of the polarization vanishes and the corresponding d_{33} of PVDF composites is lower than the d_{33} for PA11 composites.

Influence of aspect ratio of NN fillers

In this section, the influence of aspect ratio on the d_{33} (NN P's or NN NW's) is studied for different volume fractions of NN. The PVDF matrix is chosen due to an easy elaboration process.

Figure 6(b) represents the evolution of d_{33} according to the volume fraction of NN for two composites: PVDF/NN NW's and PVDF/NN P's. As expected, in both cases the d_{33} increases with the fraction of NN. d_{33} values for PVDF composites with 20 vol. % of NN are compared: in PVDF/NN P's composites, $d_{33} = 1.7$ pC.N^{-1} while for PVDF/NN NW's composite, $d_{33} = 0.8$ pC.N^{-1}. It is

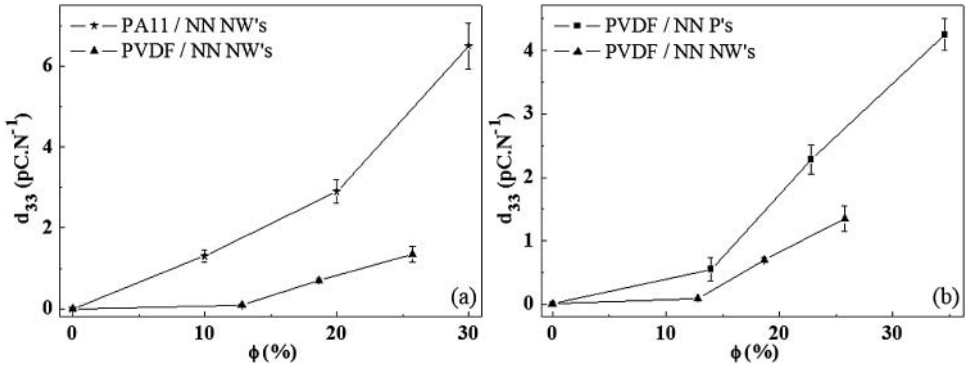

Figure 6. Variation of the piezoelectric coefficient d_{33} versus volume fraction (ϕ) of NN. (a) PA11/NN NW's and PVDF/NN NW's composites. (b) PVDF/NN NW's and PVDF/NN P's composites.

also interesting to note that d_{33} reaches 4.3 $pC.N^{-1}$ in PVDF/35 vol. % NN composite while remaining ductile.

From literature data, polymer/PZT NW's have interesting electroactive properties.[43] Unfortunately, such nanowire morphology is not adapted to NN. In the case of this study, the elaboration process does not prevent the orientation of NW's. For lead-free piezoelectric composites, polymer/NN NP's composites seem to be more adapted to reach satisfactory electroactive properties.

Conclusion

Thermoplastic/lead-free piezoelectric ceramic composites were synthesized with particles of two different morphologies: NN NW's and NN P's. XRD analyses show that both are in the orthorhombic crystalline phase, i.e. a non-centrosymmetric phase. The NN fillers were dispersed in thermoplastic matrices with different dielectric permittivities ε_M at RT: PA11 ($\varepsilon_M = 2$) and PVDF ($\varepsilon_M = 10$). The piezoelectric coefficient (d_{33}) was measured in polymer/NN NW's composites. The higher d_{33} is recorded in composites based on PA11 ($d_{33} = 6.5$ $pC.N^{-1}$ for 30 vol. % NN NW's). The vitreous state of the amorphous phase of PA11 at RT favours the piezoelectricity of PA11/NN NW's composites. The influence of the aspect ratio of the NN piezoelectric filler on PVDF/NN composites, was analysed: a higher d_{33} (2.6 $pC.N^{-1}$for 25 vol. %) is recorded in PVDF/NN P's. A more homogeneous dispersion of NN P's within the matrix might explain this result. For such NN contents, composites remain ductile. It should be noted that for hybrid composites, the piezoelectric state is reached with mild poling fields which is not the case for piezoelectric polymers. It is interesting to note that the Curie temperature of NN ceramic is higher than the processing temperature of high performance polymers. Further studies may give rise to a wide variety of multifunctional polymer/NN P's piezoelectric composites. The major interest of these composites is their ductility, easy poling and thermal stability of the piezoelectricity.

Disclosure statement

No potential conflict of interest was reported by the authors.

References

[1] Samara GA, Bauer F. The effects of pressure on the β molecular relaxation and phase transitions of the ferroelectric copolymer P(VDF0.7TrFe0.3). Ferroelectrics. 1992;135:385−399.

[2] Lee JS, Prabu AA, Kim KJ. Annealing effect upon chain orientation, crystalline morphology, and polarizability of ultra-thin P(VDF-TrFE) film for nonvolatile polymer memory device. Polymer. 2010;51:6319−6333.

[3] Tsutsumi N, Yamaoka T. Ferroelectric properties of ultrathin films of Nylon 11. Thin Solid Films. 2009;518:814−818.

[4] Takase Y, Lee JW, Scheinbeim JI, et al. High-temperature characteristics of nylon-11 and nylon-7 piezoelectrics. Macromolecules. 1991;24:6644−6652.

[5] Capsal JF, Pousserot C, Dantras E, et al. Dynamic mechanical behaviour of polyamide 11/barium titanate ferroelectric composites. Polymer. 2010;51:5207−5211.

[6] Lang SB, Muensit S. Review of some lesser-known applications of piezoelectric and pyroelectric polymers. Appl Phys A. 2006;85:125−134.

[7] Hilczer B, Szafraski M, Hilczer A. Pressure-induced changes in the dielectric response of polymer relaxors. Appl Phys Lett. 2012;100:0−4.

[8] Chen XZ, Li X, Qian XS, et al. A polymer blend approach to tailor the ferroelectric responses in P(VDF-TrFE) based copolymers. Polymer. 2013;54:2373−2381.

[9] Gan WC, Majid WHA, Furukawa T. Ferroelectric polarization, pyroelectric activity and dielectric relaxation in Form IV poly(vinylidene fluoride). Polymer. 2016;82:156−165.

[10] Tasaka S, Kawaguchi M, Inagaki N. Ferroelectric behavior in poly(β-propiolactone). Eur Polym J. 1998;34:1743−1745.

[11] Roberts S. Dielectric and piezoelectric properties of barium titanate. Phys Rev. 1947;71:890−895.

[12] Perls TA, Diesel TJ, Dobrov WI. Primary pyroelectricity in barium titanate ceramics. J Appl Phys. 1958;29:1297−1302.
[13] Teyssedre G. DSC and TSC study of a VDF/TrFE copolymer. Thermochim Acta. 1993;226:65−75.
[14] Ibos L. Contribution à l'étude de la pyroélectricité dans les polymères ferroélectriques pour capteurs intégrés [dissertation]. Toulouse (FR): University of Toulouse; 2000.
[15] Wenger MP, Das-Gupta DK. Mixed connectivity composite material characterization for electroactive sensors. Polym Eng Sci. 1999;39:1176−1188.
[16] Cross LE. Ferroelectric materials for electromechanical applications. Mater Chem Phys. 1996;34:2525−2532.
[17] Wenger MP, Almeida PL, Das-Gupta DK, et al. The ferroelectric properties of piezoelectric ceramic/polymer composites for acoustic emission sensors. Polym Eng Sci. 1999;39:483−492.
[18] Jinhua L, Ningyi Y, Chan HLW. Preparation of PCLT/P(VDF-TrFE) pyroelectric sensor based on plastic film substrate. Sens Actuators A. 2002;100:231−235.
[19] Furukawa T, Fujino K, Fukada E. Electromechanical Properties in the Composites of Epoxy Resin and PZT ceramics. Jpn J Appl Phys. 1976;15:2119−2129.
[20] Hanner KA, Safari A, Newnham RE, et al. Thin film 0−3 polymer/piezoelectric ceramic composites: Piezoelectric paints. Ferroelectrics. 1989;100:255−260.
[21] Newnham RE, Skinner DP, Cross LE. Connectivity and piezoelectric-pyroelectric composites. Mater Res Bull. 1978;13:525−536.
[22] Capsal JF, Dantras E, Dandurand J, et al. Electroactive influence of ferroelectric nanofillers on polyamide 11 matrix properties. J Non Cryst Solids. 2007;353:4437−4442.
[23] Capsal JF, Dantras E, Laffont L, et al. Nanotexture influence of BaTiO3 particles on piezoelectric behaviour of PA 11/BaTiO3 nanocomposites. J Non Cryst Solids. 2010; 356: 629−634.
[24] Hilczer B, Kulek J, Markiewicz E, et al. Dielectric relaxation in ferroelectric PZT − PVDF nanocomposites. J Non Cryst Solids. 2002;305:167−173.
[25] Lang SB, Ringgaard E. Measurements of the thermal, dielectric, piezoelectric, pyroelectric and elastic properties of porous PZT samples. Appl Phys A Mater Sci Process. 2012;107:631−638.
[26] Jain A, Prashanth KJ, Sharma AK, et al. Dielectric and piezoelectric properties of PVDF/PZT composites: a review. Polym Eng Sci. 2015;1589−1616.
[27] Directive 2002/95/EC. The European Parliament and of the Council of the European Union. Off J Eur Union. 2003;37:19−51.
[28] Mishra S, Choudhury N, Chaplot S, et al. Competing antiferroelectric and ferroelectric interactions in NaNbO3: Neutron diffraction and theoretical studies. Phys Rev B. 2007;76:024110.
[29] Yoneda Y, Fu D, Kohara S. Local structure analysis of NaNbO3. J Phys Conf Ser. 2014;502:012022.
[30] Tyunina M, Dejneka A, Rytz D, et al. Ferroelectricity in antiferroelectric NaNbO3 crystal. J Phys Condens Matter. 2014;26:125901.
[31] Moure A, Hungría T, Castro A, et al. Microstructural effects on the phase transitions and the thermal evolution of elastic and piezoelectric properties in highly dense, submicron-structured NaNbO3 ceramics. J Mater Sci. 2009;45:1211−1219.
[32] Yuzyuk YI, Simon P, Gagarina E, et al. Modulated phases in NaNbO3: Raman scattering, synchrotron X-ray diffraction, and dielectric investigations. J Phys Condens Matter. 2005;17:4977−4990.
[33] Molak A, Kubacki J. Structure of NaNbO3: xMn single crystals at room temperature. Cryst Res Technol. 2001;36:893−902.
[34] Goh GKL, Lange FF, Haile SM, et al. Hydrothermal synthesis of KNbO3 and NaNbO3 powders. J Mater Res. 2003;18:338−345.
[35] Zhu H, Zheng Z, Gao X, et al. Structural Evolution in a hydrothermal reaction between Nb2O5 and NaOH solution: from Nb2O5 grains to microporous Na2Nb2O6 2/3 H2O fibers and NaNbO3 cubes. J Am Chem Soc. 2006;128:2373−2384.
[36] Rao CNR, Deepak FL, Gundiah G, et al. Inorganic nanowires. Prog Solid State Chem. 2003;31:5−147.
[37] Marinkovic BA, Jardim PM, Morgado E, et al. Hydrothermal synthesis, crystal structure and thermal stability of Ba-titanate nanotubes with layered crystal structure. Mater Res Bull. 2008;43:1562−1572.
[38] Yuh J, Nino JC, Sigmund WM. Synthesis of barium titanate (BaTiO3) nanofibers via electrospinning. Mater Lett. 2005;59:3645−3647.
[39] Fu C, Cai W, Zhou L, et al. Synthesis of self-assembly BaTiO3 nanowire by sol-gel and microwave method. Appl Surf Sci. 2009;255:9444−9446.
[40] Joshi UA, Yoon S, Balk S, et al. Surfactant-free hydrothermal synthesis of highly tetragonal barium titanate nanowires: a structural investigation. J Phys Chem B. 2006;110:12249−12256.
[41] Joshi UA, Lee JS. Template-free hydrothermal synthesis of single-crystalline barium titanate and strontium titanate nanowires. Small. 2005;1:1172−1176.
[42] Xu CY, Zhang Q, Zhang H, et al. Synthesis and characterization of single-crystalline alkali titanate nanowires. J Am Chem Soc. 2005;127:11584−11585.

[43] Tang H, Lin Y, Andrews C, et al. Nanocomposites with increased energy density through high aspect ratio PZT nanowires. Nanotechnology. 2011;22:015702.
[44] David C, Capsal J-F, Laffont L, et al. Piezoelectric properties of polyamide 11/NaNbO3 nanowire composites. J Phys D. 2012;45:415305.
[45] Capsal JF. Elaboration et analyse des propriétés physiques de nanocomposites hybrides ferroélectriques [dissertation]. Toulouse (FR): University of Toulouse; 2008.
[46] Ploss B, Ploss B, Shin FG, et al. Pyroelectric or piezoelectric compensated ferroelectric composites. Appl Phys Lett. 2000;76:2776−2778.
[47] Dias CJ, Das-Gupta DK. Ferroelectric ceramic polymer composite films for pyroelectric sensors. IEEE Trans Dielectr Electrical Insulation. 1996;3:393−396.
[48] Golding D. Metastable ferroelectric sodium niobate. J Am Ceram Soc. 1964;4:1962−1965.
[49] Pan H, Zhu G, Chao X, et al. Properties of NaNbO3 powders and ceramics prepared by hydrothermal reaction. Mater Chem Phys. 2011;126:183−187.
[50] Liu XF, Xiong CX, Sun HJ, et al. Piezoelectric and dielectric properties of PZT/PVC and graphite doped with PZT/PVC composites. Mater Sci Eng B. 2006;127:261−266.